Acute skin exposure to ultraviolet light triggers neutrophil-mediated kidney inflammation

Sladjana Skopelja-Gardner[a,1], Joyce Tai[a], Xizhang Sun[a], Lena Tanaka[a], James A. Kuchenbecker[b], Jessica M. Snyder[c], Paul Kubes[d], Tomas Mustelin[a,e], and Keith B. Elkon[a,e,f,1]

[a]Division of Rheumatology, University of Washington, Seattle, WA 98195; [b]Department of Ophthalmology, University of Washington, Seattle, WA 98195; [c]Department of Comparative Medicine, University of Washington, Seattle, WA 98195; [d]Calvin, Phoebe and Joan Snyder Institute for Chronic Diseases, University of Calgary, Calgary, AB T2N 1N4, Canada; [e]Center for Innate Immunity and Immune Disease, University of Washington, Seattle, WA 98195; and [f]Department of Immunology, University of Washington, Seattle, WA 98195

Edited by Jason G. Cyster, University of California, San Francisco, CA, and approved December 2, 2020 (received for review September 16, 2020)

Photosensitivity to ultraviolet (UV) light affects up to ~80% of lupus patients. Sunlight exposure can exacerbate local as well as systemic manifestations of lupus, including nephritis, by mechanisms that are poorly understood. Here, we report that acute skin exposure to UV light triggers a neutrophil-dependent injury response in the kidney characterized by upregulated expression of endothelial adhesion molecules as well as inflammatory and injury markers associated with transient proteinuria. We showed that UV light stimulates neutrophil migration not only to the skin but also to the kidney in an IL-17A–dependent manner. Using a photoactivatable lineage tracing approach, we observed that a subset of neutrophils found in the kidney had transited through UV light–exposed skin, suggesting reverse transmigration. Besides being required for the renal induction of genes encoding mediators of inflammation (*vcam-1*, *s100A9*, and *Il-1b*) and injury (*lipocalin-2* and *kim-1*), neutrophils significantly contributed to the kidney type I interferon signature triggered by UV light. Together, these findings demonstrate that neutrophils mediate subclinical renal inflammation and injury following skin exposure to UV light. Of interest, patients with lupus have subpopulations of blood neutrophils and low-density granulocytes with similar phenotypes to reverse transmigrating neutrophils observed in the mice post-UV exposure, suggesting that these cells could have transmigrated from inflamed tissue, such as the skin.

UV light | neutrophil migration | kidney | inflammation

Sensitivity to ultraviolet (UV) sunlight rays is a well-recognized feature of systemic lupus erythematosus (SLE) (1). Skin exposure to UV light triggers both local and systemic inflammation and has been associated with systemic disease flares, including lupus nephritis (LN), in SLE patients (2–4). How photosensitivity in the skin leads to systemic manifestations remains poorly understood. Shared gene signatures in the skin and kidney of SLE patients (5) suggest common pathogenesis. We recently observed that acute skin exposure to UV light triggers both a local and a systemic type I interferon (IFN-I) response (6), indicating inflammatory responses to UV light are not limited to the skin. How exactly skin exposure to UV light impacts the kidney is not known.

We and others have shown that UV light induces rapid neutrophil infiltration into the skin (6, 7). Although neutrophils are major contributors to inflammation at local injury sites, it has recently been recognized that neutrophils can also home to organs distant from the primary site of inflammation (8–10), where they contribute to lung tissue injury via production of reactive oxygen species (ROS) (11) or activate the adaptive immune system in the lymph nodes and the bone marrow (9, 12). In SLE, neutrophils are thought to play an important role in both local and systemic disease. Neutrophils are present in the skin lesions of SLE patients (13, 14) and in the kidney tissue of patients with LN (15, 16). High expression of a neutrophil gene signature is a strong predictor of active disease, including LN and cutaneous flares (17, 18). Proinflammatory low-density granulocytes (LDGs) are increased particularly in patients with skin disease (19). While these findings implicate neutrophils in local tissue injury in SLE, whether neutrophils provide the pathogenic link between skin inflammation and kidney injury is not understood.

To elucidate how skin exposure to UV light impacts the kidney and the role neutrophils play in these processes, we evaluated changes in renal gene expression in concert with neutrophil migration. We found that acute skin exposure to UV light stimulates inflammatory processes in the kidney, including expression of endothelial adhesion molecules, inflammatory mediators, injury markers, and transient proteinuria. Notably, we found that neutrophils migrated to the kidney after UV light exposure in an IL-17A–dependent manner, localizing to the tubulointerstitial (TI) areas where they exhibited proinflammatory phenotypes. Blocking neutrophil trafficking by anti–G-CSF immunoglobulin (IgG) treatment abrogated renal inflammation and prevented up-regulation of tubular injury markers. Together, these findings demonstrate that skin exposure to UV light triggers subclinical renal inflammatory and injury processes mediated by neutrophils.

Results

Skin Exposure to UV Light Causes Subclinical Kidney Injury. Exposure to sunlight has been associated with aggravation of systemic symptoms and occurrence of disease flares in SLE patients, including nephritis (2–4). Therefore, we first asked whether acute sterile inflammation in the skin triggered by a single exposure to

Significance

Neutrophils are the most abundant leukocytes in circulation and the first responders to infectious and sterile inflammation, including skin exposure to ultraviolet (UV) light. We demonstrate that neutrophils not only migrate to the UV light–exposed skin but also disseminate systemically. In the kidney, neutrophils mediate inflammatory and injury responses triggered by skin exposure to UV. They had a proinflammatory phenotype: increased production of reactive oxygen species and a subpopulation of neutrophils in the kidney extravasated from UV light-exposed skin tissue. These studies demonstrate a direct link between skin inflammation by UV light and kidney injury and implicate neutrophils as pathogenic mediators, therefore providing a model by which exposure to UV light might contribute to kidney damage in lupus patients.

Author contributions: S.S.-G., J.A.K., P.K., T.M., and K.B.E. designed research; S.S.-G., J.T., X.S., and L.T. performed research; J.A.K. contributed new reagents/analytic tools; S.S.-G., J.T., and J.M.S. analyzed data; and S.S.-G., T.M., and K.B.E. wrote the paper.

The authors declare no competing interest.

This article is a PNAS Direct Submission.

[1]To whom correspondence may be addressed. Email: ssg12@uw.edu or KElkon@medicine.washington.edu.

This article contains supporting information online at https://www.pnas.org/lookup/suppl/doi:10.1073/pnas.2019097118/-/DCSupplemental.

Published January 4, 2021.

ultraviolet B (UVB) light (500 mJ/cm^2) in black 6 (B6) mice leads to changes in the kidney, including inflammation, injury, and proteinuria (Fig. 1*A*). The lung was chosen as a control organ, as no association between photosensitivity and clinical lung disease has been reported in SLE. A total of 500 mJ/cm^2 of UVB light in B6 mice has been defined as two minimal erythematous doses (20), the reference dose used for human phototesting (21). Gene expression analyses of perfused kidney tissues (Fig. 1*A*) revealed up-regulation in the gene expression of adhesion molecules *vcam-1* and *e-selectin* on days 1 and 2 after UVB light exposure (Fig. 1 *B* and *C*). In contrast, *vcam-1* and *e-selectin* expression demonstrated a downward trend in the lung (*SI Appendix*, Fig. S1). We also observed a >10-fold renal induction in *s100A9*, a neutrophilic mediator associated with kidney damage (22), as well as increased *s100A6* expression, a calcium-binding protein associated with tubular injury (23) (Fig. 1 *D* and *E*). While *s100A9* induction was detected in the lung, *s100A6* gene expression remained unchanged in the lung (*SI Appendix*, Fig. S1). The inflammatory response in the kidney was also associated with an early increase in *il-1β* expression (days 1 and 2 after UV), whereas there was minimal or no change in *tnf* or *il-6* (Fig. 1*F*). *Il-1β* expression was not detected in the lung until 6 d after skin exposure to UVB light (*SI Appendix*, Fig. S1). Rapid induction in *cxcl12* expression, a chemokine secreted by glomeruli and tubules and implicated in renal injury (24), was also found in the kidney but not the lung (Fig. 1*G* and *SI Appendix*, Fig. S1). Therefore, UVB light–triggered skin injury instigates rapid renal proinflammatory processes, while fewer changes are observed in the lung.

In addition to the proinflammatory response observed in the kidney, both proteinuria and the urinary albumin/creatinine ratio increased in the first few days after skin exposure to UVB light (Fig. 1 *H* and *I*). This rapid effect on kidney function was

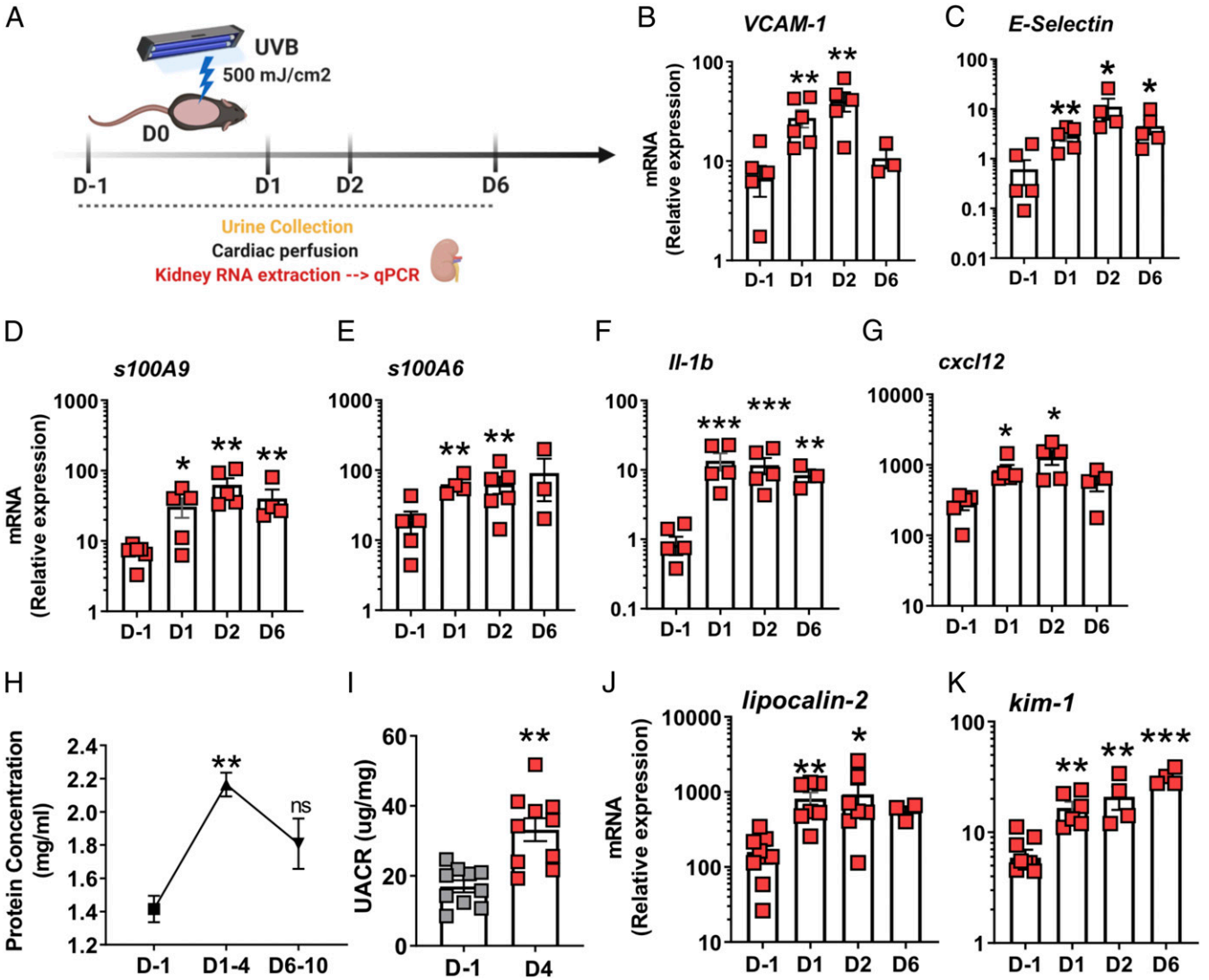

Fig. 1. Skin exposure to UVB light triggers kidney inflammatory responses, transient proteinuria, and up-regulation of kidney injury markers. (*A*) Following skin exposure to a single dose of UVB light (500 mJ/cm^2), urine and kidney samples were collected at the time points shown (D = day) following cardiac perfusion. (*B*–*G*) Gene expression of (*B* and *C*) adhesion molecules *vcam-1* and *e-selectin* and (*D*–*G*) inflammatory mediators *s100a9*, *s100a6*, *il1b*, and *cxcl12* on different days following exposure to UVB light relative to the non-UV–irradiated controls (D-1) was determined by qPCR. Significance was determined by one-way ANOVA with Tukey's post hoc (n = 3 to 6 per group; *P < 0.05, **P < 0.01, ***P < 0.001). (*H* and *I*) Proteinuria was quantified by (*H*) Bradford assay and (*I*) urine albumin/creatinine ratio (UACR) at the times shown after exposure to UV light. Significant differences in proteinuria/UACR were determined relative to measurements from the urine of nonirradiated controls (D-1) using (*H*) one-way ANOVA with Tukey's post hoc or (*I*) Student's t test (n = 10 per time frame; **P < 0.01). (*J* and *K*) Gene expression of renal endothelial injury markers (*J*) *lipocalin-2* and (*K*) *kim-1* over time following skin exposure to UV light was compared to non-UV–exposed controls (D-1). Significance was determined by one-way ANOVA with Tukey's post hoc (n = 3 to 6 per group; *P < 0.05, **P < 0.01, ***P < 0.001).

accompanied by up-regulation in the expression of *lipocalin-2* and kidney injury molecule 1 (*kim-1*) (Fig. 1 *J* and *K*), markers of tubular kidney damage that are also observed in LN (25, 26). Despite the transient nature of proteinuria, expression of these kidney injury markers persisted up to day 6 (Fig. 1 *J* and *K*), possibly reflecting tissue repair.

UV Light–Induced Inflammation in the Skin Results in Neutrophil Migration to the Kidney. To investigate whether neutrophils participate in the systemic inflammatory response to UVB light, we examined the kinetics of neutrophil accumulation in UV light–irradiated skin as well as in the spleen, kidney, and lung of C57BL/6 J (B6) mice, a strain that best mimics cutaneous changes to UVB light in human skin (Fig. 2*A*) (27). Following acute skin exposure to UVB light, neutrophil numbers in the skin increased sevenfold within 24 h and remained elevated for 6 d compared to baseline pre-UV levels (D-1) (Fig. 2*B*). This was accompanied by a reduction in neutrophil numbers in the bone marrow and a fivefold increase in circulating blood neutrophils on days 1 to 6 (Fig. 2 *C* and *D*). Intriguingly, in the same time frame, neutrophils increased in the spleen, lung, and kidney (Fig. 2 *E*–*G* and *SI Appendix*, Fig. S2*A*). The precise kinetics varied between organs, reaching peak on day 1 in the lung and days 2 to 6 in the kidney and spleen (Fig. 2 *E*–*G*). In the kidneys, neutrophils mostly localized to the tubulointerstitial area, including the vasculature, as indicated by neutrophil elastase (NE) staining in proximity to, or colocalized with, platelet/endothelial cell adhesion molecule-1 (PECAM-1/CD31) (Fig. 2*H*). Representative images in Fig. 2*H* show neutrophils in or around the interstitial vasculature (full white arrows) and in the interstitium (dotted white arrows), with occasional neutrophils also found in the glomeruli (yellow arrows). Similar localization was detected with anti-Ly6G immunofluorescence (IF) staining (*SI Appendix*, Fig. S2*B*).

To determine whether other innate immune cells showed local and systemic responses similar to neutrophils, we examined the distribution of monocytes (CD11b+Ly6C+Ly6G−) at the same time points after UVB light exposure. While monocytes were also recruited into the skin, only small numbers of infiltrating monocytes were detected in the kidney on day 6 after UVB exposure (~2-fold versus ~10.5-fold increase in kidney neutrophils) (Fig. 2*F* and *SI Appendix* Fig, S3). No increase in monocyte numbers was detected in the lung or spleen (*SI Appendix*, Fig. S3), suggesting that the systemic response to UV injury was relatively selective for neutrophils.

Infiltration of neutrophils into the skin was accompanied by histologic changes, including early inflammation of the dermis and epidermal cell death (days 1 and 2), followed by development of acanthosis and hyperkeratosis with serocellular crust formation in some cases (day 6) (*SI Appendix*, Fig. S4). Notably, no open skin lesions appeared after exposure to UVB light, suggesting that the observed immune cell infiltration occurred under sterile conditions, although a contribution by an altered skin microbiome cannot be excluded (20).

Together, these findings demonstrate that exposure of the skin to a single dose of UVB light mobilizes neutrophils to both the local site of inflammation as well as to internal organs, including the kidney, accompanied by blood neutrophilia. While overall migratory patterns were similar in both male and female mice, neutrophil infiltration into the skin was more rapid in females compared to males (Fig. 2*B*). In contrast, epidermal injury by tape stripping did not lead to neutrophil migration to the kidney despite similar levels of neutrophil infiltration and inflammatory response and tissue injury as seen with UV light exposure (*SI Appendix*, Fig. S5), indicating that systemic neutrophil dissemination is not common to all forms of sterile skin injury.

IL-17A Promotes Neutrophil Recruitment following Skin Exposure to UV Light. A survey of chemotactic and inflammatory mediators in the skin revealed significant up-regulation of the gene expression of neutrophil chemokines and inflammatory cytokines *cxcl1*, *cxcl5/6*, *g-csf*, and *il-1β* 1 to 2 d after UV exposure (Fig. 3 *A*–*D*). The rapid and persistent increase in expression of *s100A9* matched the kinetics of neutrophil infiltration into the skin (Fig. 2*B* and *SI Appendix*, Fig. S6), whereas the cytokines *il-6*, *tnf*, and *il-33* were transiently increased and returned to baseline expression by day 6 (*SI Appendix*, Fig. S6). In contrast, *il-36a* was elevated only on day 6 (*SI Appendix*, Fig. S6), perhaps reflecting a reparative function. The transient (1 to 2 d) presence of monocytes in the skin (*SI Appendix*, Fig. S3) paralleled the up-regulation of monocyte-specific chemokines *ccl4* and *ccl2* (*SI Appendix*, Fig. S6). Similar to the accumulation of neutrophils in the skin of female mice (Fig. 2*B*), monocyte accumulation in the skin also occurred earlier in females than males (*SI Appendix*, Fig. S3).

UV skin exposure was accompanied by rapid (6 h) 12-fold induction in *il-17a* gene expression in the skin (Fig. 3*E*) as well as >1,000-fold cutaneous induction in *g-csf* expression during days 1 and 2 after UV (Fig. 3*C*). To determine whether the induction of these cytokines was relevant to neutrophil mobilization, we first quantified cytokine protein concentrations in the blood, which revealed a robust and sustained (10- to 100-fold) increase in the concentration of plasma IL-17A 6 to 24 h after exposure to UV light (Fig. 3*F*), together with a transient (peak at 6 h) increase in IL-6 and IL-12, cytokines that may be downstream of IL-17A (28) (Fig. 3 *G* and *H*). No increase in the plasma concentrations of IFNγ, GM-CSF, TNFα, IL-10, IL-27, IL-23, or IL1α were observed.

To determine if IL-17A is necessary for UVB-induced neutrophil recruitment, we blocked the effect of IL-17A with a neutralizing antibody prior to UV exposure (Fig. 3*I*). Anti–IL-17A IgG significantly dampened blood neutrophilia (Fig. 3*J*) and attenuated neutrophil influx into both the exposed skin tissue (Fig. 3*K* and *SI Appendix*, Fig. S7*A*) and the kidney (Fig. 3*L* and *SI Appendix*, Fig. S7*B*). These findings demonstrate neutrophil recruitment in response to UV light is mediated, at least in part, by IL-17A.

Neutrophils Mediate Kidney Inflammation after Skin Exposure to UV Light. To determine whether neutrophils were responsible for the inflammatory changes in the kidney following skin UVB light exposure, we blocked neutrophil recruitment prior to UV light exposure. Since cutaneous *g-csf* expression was up-regulated >1,000-fold after UV exposure, suggesting a chemotactic role for G-CSF in neutrophil recruitment in response to UV light, we inhibited neutrophil mobilization from the bone marrow by blocking G-CSF as outlined in Fig. 4*A*. Neutralizing G-CSF prevented blood neutrophilia as well as neutrophil recruitment to the kidney after skin exposure to UVB light (Fig. 4 *B* and *C*). Notably, as previously reported in different models (29, 30), blocking G-CSF did not alter monocyte numbers in the kidney (Fig. 4*D*). Decreased neutrophil migration to the kidney was accompanied by a significant reduction in the renal expression of the adhesion molecules *vcam-1* and *e-selectin* (Fig. 4 *E* and *F*) as well as the inflammatory mediators *s100A9* and *il-1β* 1 d after UVB exposure (Fig. 4 *G* and *H*). Furthermore, the tissue injury markers *lipocalin-2* and *kim-1* in the kidney were significantly decreased in UV light–exposed mice treated with G-CSF blocking antibody relative to isotype-treated UV-exposed animals (Fig. 4 *I* and *J*). As we reported previously (6), acute skin exposure to UVB light triggered a type I interferon response in the kidney (Fig. 4*K*). Blocking G-CSF significantly reduced, but did not completely abrogate, the IFN score (Fig. 4*K*). While the presence of neutrophils in the kidney was required for the acute inflammatory and injury responses observed 1 d after skin UV light exposure (Fig. 4), no differences in proteinuria were seen at this time point, as peak proteinuria occurred around day 4 after UV exposure (Fig. 1 *H* and *I*). Together, these data indicate that neutrophils are responsible for the inflammatory response and, directly or indirectly, contribute to type I interferon induction in the kidney following UV light exposure of the skin. Similar to the results obtained with anti–G-CSF IgG, administration of a neutralizing

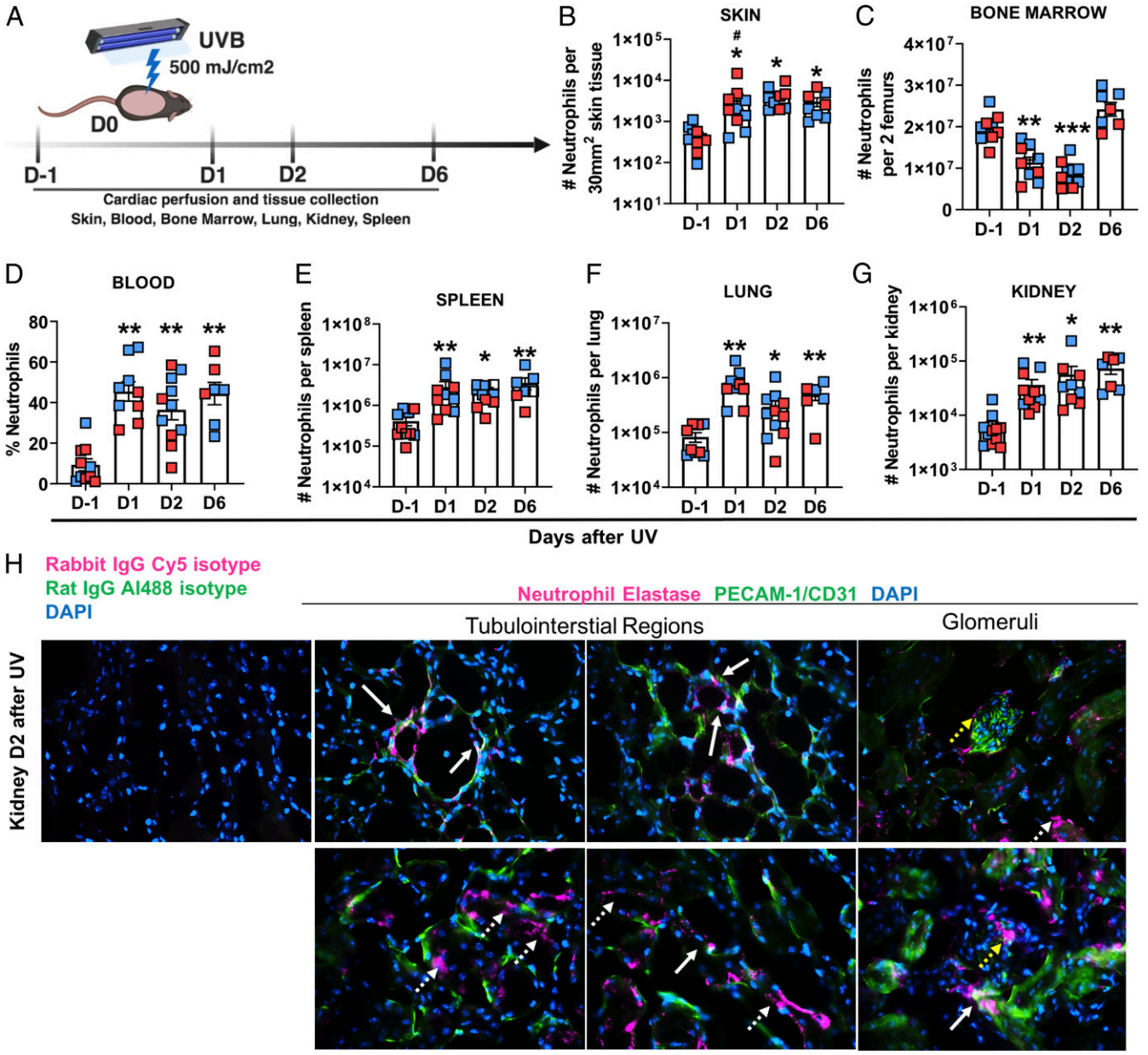

Fig. 2. Skin exposure to UVB light triggers neutrophilia and neutrophil infiltration into the skin and peripheral organs, including the kidney. (*A*) Following a single exposure of skin to 500 mJ/cm^2 UVB light, neutrophils were quantified in the blood, skin, lung, spleen, and kidney at the time points shown. Following whole body perfusion, cells were isolated from the sites shown in *B*–*G*, and the number of neutrophils (Ly6C+Ly6G+ cells) evaluated in the CD45+ live cells gate in female (red) and male (blue) mice on days (D) 1, 2, and 6 after UV exposure. Differences in neutrophil numbers on different days after exposure to UVB light were determined relative to nonirradiated controls (D-1) using one-way ANOVA with Tukey's post hoc (n = 6 to 10 per group; mean ± SEM; $^*P < 0.05$, $^{**}P < 0.01$, $^{***}P < 0.001$; $^{\#}P < 0.05$ comparing fold increase in male versus female mice). Representative flow cytometry plots for each organ are shown in *SI Appendix*, Fig. S5. (*H*) IF staining of frozen kidney sections on D2 after UV exposure demonstrating NE (Cy5, magenta), PECAM-1/CD31 (Al488, green), and nuclear DAPI (blue) staining in the tubulointerstitium and glomeruli. NE staining in vascular endothelium is denoted by a white, full arrow (colocalization of NE and CD31, yellow); NE staining in the interstitial tissue is denoted by dotted white arrows; and NE staining in glomeruli is denoted by yellow arrows. Isotype control staining is shown in the leftmost panel. (Magnification, 40×.)

anti–IL-17 antibody partially suppressed neutrophil migration to the kidney and resulted in decreased gene expression of kidney inflammatory (*vcam-1* and *s100A9*) and injury markers (*lipocalin-2* and *kim-1*), although only the reduction in *kim-1* expression was statistically significant (*SI Appendix*, Fig. S7 *C*–*F*).

A Subpopulation of Kidney Neutrophils Is Reverse Transmigrated, a Phenotype Also Detected in the Blood of SLE Patients. While it has long been assumed that neutrophils entering sites of infection or sterile inflammation subsequently undergo apoptosis and are rapidly removed by macrophages, a number of studies have revealed that some neutrophils traffic in a bidirectional manner, that is, after entering a tissue, they transmigrate back into the bloodstream and infiltrate another location, a process referred to as reverse transmigration (rTEM) (8, 10, 11, 31–34). To investigate whether neutrophils that homed to the kidney after skin exposure to UVB light transited via the exposed skin, we studied neutrophil migration in a photoactivatable B6 mouse model (human ubiquitin C [UBC]-photoactivated [PA]-green fluorescent protein [GFP]).

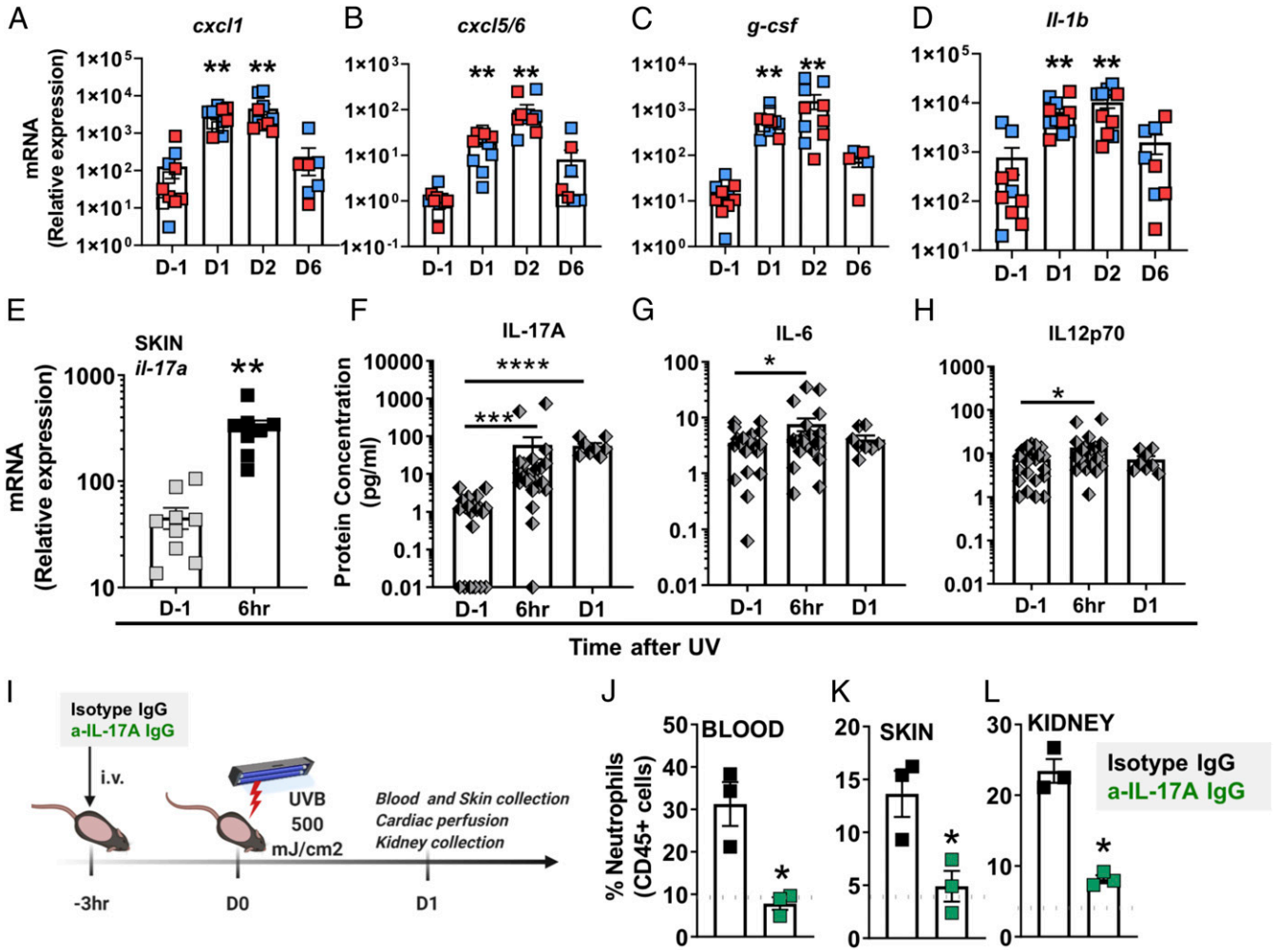

Fig. 3. Skin exposure to UV light triggers IL-17A production, which is required for neutrophil recruitment. (*A–D*) Relative mRNA expression in skin obtained from female (red) and male (blue) mice was quantified by qPCR using the primers listed in *SI Appendix*, Table S1 and normalized to *18S* transcript levels. The bars represent mean relative expression ± SEM for all samples combined. (*E*) *Il-17A* gene expression in the skin 6 h after UV exposure was quantified as in *A–D*. (*F–G*) Multiplex analysis of the protein concentration in plasma samples collected 6 h or one day (D1) after UV (*F*) IL-17A, (*G*) IL-6, and (*H*) IL-12p70. Significant changes in gene expression and plasma protein levels at different time points after exposure to UV light were determined relative to those of nonirradiated controls (D-1) using one-way ANOVA with Tukey's post hoc (*A–D*, $n = 8$ to 10; *F–H*, $n = 8$ to 25 mice per group; mean ± SEM, $^*P < 0.05$, $^{**}P < 0.01$, $^{***}P < 0.001$). (*I*) Shaved B6 mice were treated intravenously (i.v.) with 100 μg anti–IL-17A IgG (green) or isotype control IgG (black) 3 h before exposure to a single dose of UVB light (500 mJ/cm^2). One day after UV exposure (D1), neutrophils were quantified in (*J*) blood, (*K*) skin, and (*L*) kidney by flow cytometry as in Fig. 2. The dotted gray lines represent the average baseline neutrophil percentage in blood, skin, and kidney of noninjected mice. Statistical differences between treatment groups were determine by paired Student's *t* test ($n = 3$, $^*P < 0.05$, $^{****}P < 0.0001$).

The experimental scheme is illustrated in Fig. 5*A*; 1 d after skin exposure to a single dose of UVB light, the skin was exposed to violet light (405 nm) such that infiltrating immune cells were photoconverted to GFP-positive cells. Photoconverted neutrophils (GFP+Ly6G+) were then quantified in perfused kidneys the next day. Flow cytometry analysis revealed that ∼20% of kidney-infiltrating neutrophils were GFP positive after subtraction of background signal (∼10%) (Fig. 5*B*). In contrast to the models of sterile inflammation in the liver or cremaster muscle (8, 10), we did not detect photoconverted neutrophils in the lung, possibly because few neutrophils were found in the lung on day 2 (Fig. 2*F*). To test whether GFP+ neutrophils in the kidney extravasated from UV-exposed skin tissue or were PA intravascularly, we compared the changes in the numbers of GFP+ neutrophils obtained from the kidneys of mice in which the same skin that was exposed to UV light was PA with violet light a day later (Group I) versus mice in which the skin adjacent to that exposed to UV light was PA with violet light a day later (Group II, diagram in *SI Appendix*, Fig. S8*A*). Although there were no differences in the percentages of circulating neutrophils between the groups (*SI Appendix*, Fig. S8*B*), a greater increase in GFP+ neutrophils was observed in the kidneys of mice where UV-exposed skin was also PA (Group I) compared to the lack of increase in GFP+ neutrophils in the mice where non-UV–exposed skin was PA (Group II) (*SI Appendix*, Fig. S7*B*). In Group II, the neutrophil numbers were similar to the background of GFP positivity seen in Fig. 5*B* (*SI Appendix*, Fig. S8*B*).

While low levels of GFP+ kidney neutrophils in Group II suggested that violet light did not PA circulating cells in non-UV–exposed skin, it remained possible that exposure to UV light altered neutrophil interactions with blood vessels in the skin, allowing for greater photoconversion and subsequent kidney access. To determine the relative proportions of rTEM neutrophils, we quantified the expression of surface markers used to characterize neutrophils that underwent rTEM: CXCR4^{hi} (8) and ICAM1^{hi}CXCR1^{lo} (11, 35). Indeed, GFP+ kidney neutrophils expressed higher levels of CXCR4 compared to GFP+ neutrophils in the skin or GFP− neutrophils in the kidney (Fig. 5*C*). Of

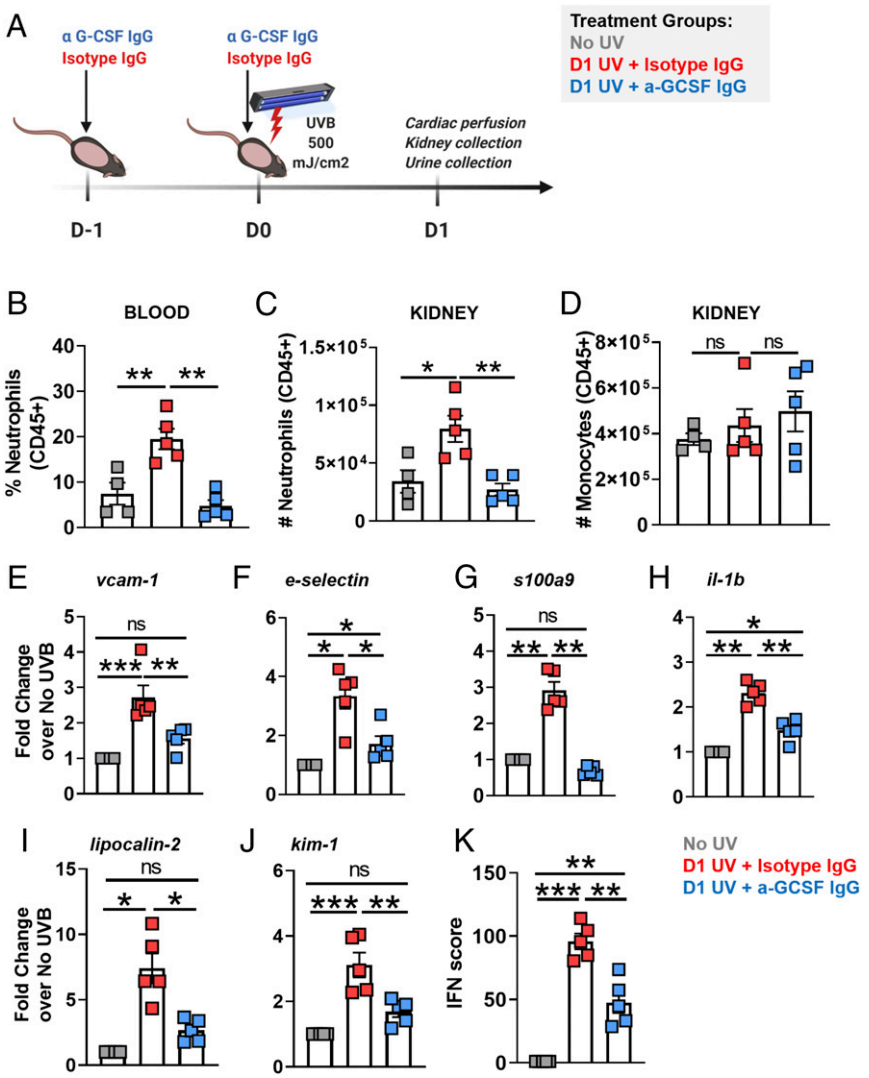

Fig. 4. UVB light–triggered neutrophil migration to the kidney is required for kidney inflammatory and injury responses. (*A*) B6 mice ($n = 4$ to 5 per group) were either not exposed to UV (no UV, gray), were exposed to UV and received 50 μg isotype control IgG intraperitoneally (i.p.) (red), or were exposed to UV and received 50 μg anti-GCSF IgG i.p. (blue). Two doses of anti–G-CSF blocking IgG or isotype control IgG were given at 24 h and 3 h prior to UVB skin exposure. One day after UV exposure (D1), kidneys were collected and analyzed by flow cytometry and qPCR. (*B–D*) Flow cytometry analysis of (*C*) percent neutrophils (CD11b+Ly6C+Ly6G+) in the blood, (*D*) number of neutrophils per kidney, and (*E*) number of monocytes (CD11b+Ly6C+Ly6G−) in the CD45+ kidney cell population. (*E–J*) Gene expression analysis of (*E* and *F*) adhesion molecules *vcam-1* and *e-selectin*, (*G* and *H*) inflammatory mediators *s100a9* and *il1b*, and (*I* and *J*) kidney injury markers *lipocalin-2* and *kim-1*. (*K*) IFN-I score in the kidney was evaluated based on relative expression of 10 ISGs as described in *Materials and Methods*. (*B–K*) Statistical significance was determined by one-way ANOVA with Tukey's post hoc ($n = 4$ to 5 per group; mean ± SEM, $*P < 0.05$, $**P < 0.01$, $***P < 0.001$, ns = not significant).

interest, renal expression of the CXCR4 ligand, *cxcl12*, 1 to 2 d after skin exposure to UVB light was concurrent with the presence of CXCR4^{hi} neutrophils in the kidney (Fig. 1*G*), possibly providing the chemotactic stimulus for recruitment of these neutrophils into the kidney. Of interest, we detected CXCR4^{hi} and ICAM1-^{hi}CXCR1^{lo} neutrophils in the bone marrow late after UV exposure (day 6, *SI Appendix*, Fig. S9 *B* and *C*), suggesting that some of these neutrophils also home back to the bone marrow similar to what has been reported for rTEM following liver injury or virus infection of the skin (12, 36). Consistent with these observations, we detected higher CXCR4 expression on blood neutrophils on day 2 after UV exposure, possibly capturing cells en route to the kidney and bone marrow (*SI Appendix*, Fig. S9*D*).

Similarly, a significantly greater percentage of ICAM1^{hi}CXCR1^{lo} cells was detected among the GFP+ neutrophils in the kidney compared to GFP+ neutrophils in the skin and GFP− neutrophils in the kidney (Fig. 5*D*). The ICAM1^{hi}CXCR1^{lo} phenotype was detected on ∼20 to 35% of GFP+ neutrophils in the kidney (Fig. 5*D*), suggesting that a subset of neutrophils that migrate to the kidney via UV-exposed skin do so by reverse transmigration, whereas the remainder of kidney neutrophils are likely activated while circulating through inflamed UV-exposed skin. The ICAM1-^{hi}CXCR1^{lo} neutrophil subpopulation was also detected in the kidneys of normal B6 mice exposed to UV light that did not receive PA (*SI Appendix*, Fig. S9*A*).

While both CXCR4^{hi} and ICAM1^{hi}CXCR1^{lo} neutrophil phenotypes have been associated with inflammatory functions and tissue injury in different murine models (11, 31, 37), few studies have been performed on these cell populations in human disease. Given the emerging role of neutrophils in SLE (13, 17, 18) and their apparent heterogeneity (19), we investigated whether normal-density polymorphonuclear cells (PMNs) or LDGs from SLE patients

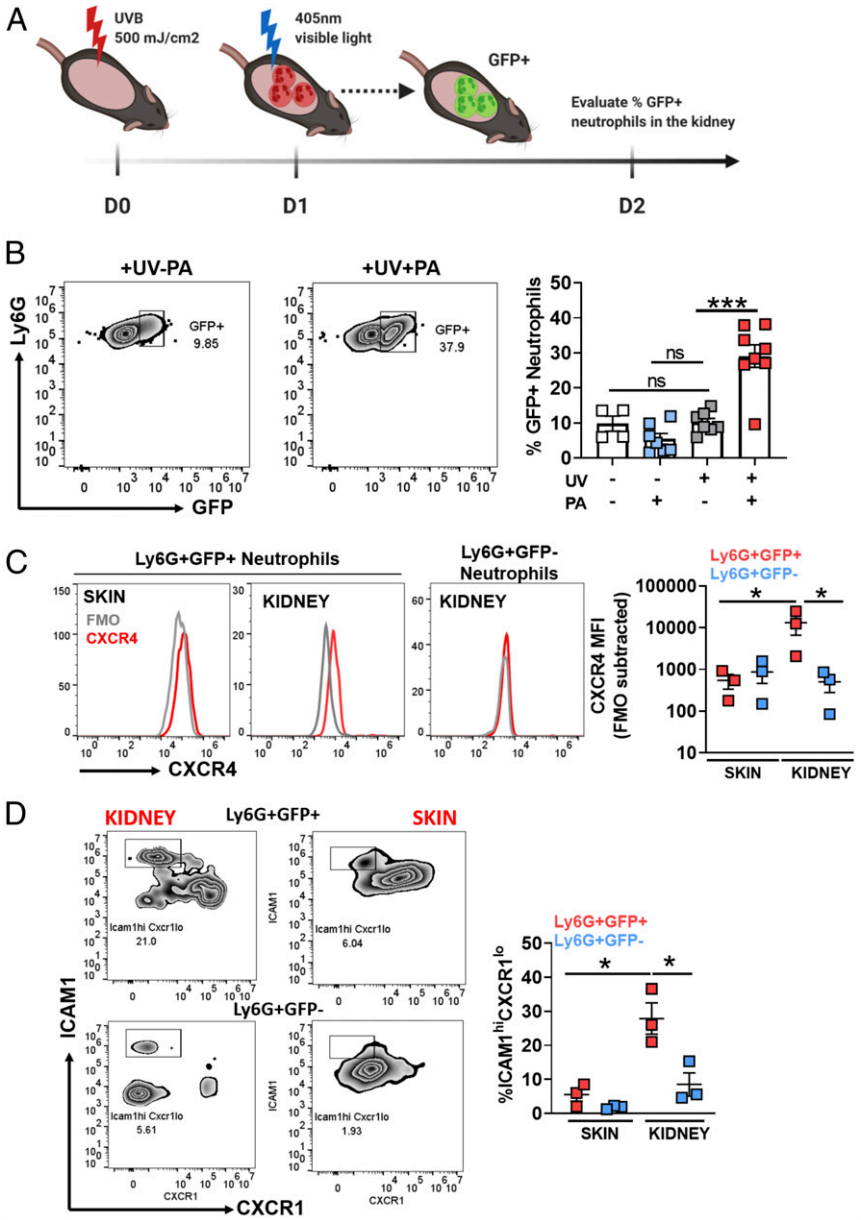

Fig. 5. A subpopulation of kidney neutrophils are derived from UV light–exposed skin. (*A*) UBC-PA-GFP mice were shaved and irradiated with UVB light as in Fig. 1. One day (D1) after UV exposure, the UV-irradiated skin was subjected to PA by violet light (405 nm), as described in *Materials and Methods*. Cardiac perfusion was performed and kidneys collected 24 h after PA (D2). (*B*) The percentage of GFP+ neutrophils (CD45+Ly6C^{int}Ly6G^{hi}) in the kidneys of UV-exposed (UV+) and PA (PA+) mice was determined by flow cytometry. The percentage of GFP+ neutrophils was compared to the kidneys from three different mouse controls: no UV, no PA; no UV, +PA; and +UV, no PA by one-way ANOVA with Tukey's post hoc ($n = 4$ to 8 animals/treatment, $***P < 0.001$, ns = not significant). (*C*) CXCR4 mean fluorescence intensity (MFI) was determined by flow cytometry in photoconverted (GFP+, red) neutrophils in the skin and kidney and GFP– (blue) neutrophils in the skin and kidney of mice exposed to UV light and PA as shown in *A*. Skin and kidney tissue were analyzed at the same time. The MFI was determined by subtracting FMO MFI for each tissue. (*D*) Flow cytometry analysis of the percent ICAM1^{hi}CXCR1^{lo} cells in the GFP+ and GFP– neutrophil populations in the skin and kidneys of mice exposed to UV light and PA as shown in *A*. (*C* and *D*) Statistical differences between groups were determined by Student's *t* test ($n = 3$ individual experiments; $*P < 0.05$).

demonstrated the reverse migrating phenotypes: CXCR4^{hi} (37, 38) and ICAM1^{hi}CXCR1^{lo}. Flow cytometry profiling of PMNs and LDGs revealed higher CXCR4 expression on the surface of these cells in SLE patients compared to healthy controls (Fig. 6 *A* and *C*). Moreover, we found a small but significantly higher percentage of ICAM1^{hi}CXCR1^{lo} PMNs in SLE blood (mean, 3.5%) relative to healthy controls (mean, 1.4%) (Fig. 6*B*). Interestingly, the LDG neutrophil population (CD15^{+}CD14^{lo}CD10^{+} in peripheral blood mononuclear cells [PBMCs]) contained a greater percentage of ICAM1^{hi}CXCR1^{lo} cells than the PMNs in both healthy (mean, 7.1%) and SLE blood (mean, 29.4%) (Fig. 6 *B* and *D*). The rTEM-like population was significantly more highly represented in LDGs from SLE patients relative to healthy controls (Fig. 6*D*). These data identify the presence of rTEM-like neutrophil phenotypes in PMNs and particularly LDGs in SLE patients.

Discussion

The systemic effects of skin exposure to UV light are poorly understood. Identifying these pathways in normal baseline conditions may inform mechanisms of systemic tissue involvement after sun

exposure that occurs in diseases such as SLE (2–4). Here, we report several findings on how exposure to sunlight impacts the kidney. First, we demonstrated that acute skin exposure to UVB light triggers inflammatory and injury responses in the kidney, including subclinical proteinuria. Intriguingly, these renal changes were accompanied by neutrophil infiltration into the kidney following UVB light–mediated skin inflammation. The neutrophil response was dependent on IL-17A and G-CSF. Neutrophils in the kidney had proinflammatory phenotypes, as evidenced by extracellular localization of NE, a higher proportion of rTEM ($CXCR4^{hi}$) also known as "aged" and $ICAM1^{hi}CXCR1^{lo}$ cells. Neutrophils were directly implicated in subclinical kidney injury, as neutrophil depletion resulted in significant reductions in the expression of adhesion molecules, inflammatory cytokines, IFN-I signature, and kidney injury markers after skin UV exposure.

Other types of skin injury, such as tape stripping and topical application of a TLR7 agonist, have been reported to enhance kidney injury in certain lupus models, although disease enhancement was thought to be mediated by macrophages and dendritic cells rather than neutrophils (39, 40). Having demonstrated that tape stripping did not lead to neutrophil recruitment to the kidney, we propose that UV light exposure is different from other types of sterile skin inflammation. This may be explained by the generation of photoproducts or unique inflammatory mediators after UV injury that prime the kidney for inflammation, by differences in removal of neutrophils after UV compared with tape stripping, or by other factors. We observed that UV light triggered a rapid and strong induction of *il-17a* messenger RNA (mRNA) in the skin together with high circulating IL-17A protein levels (~100-fold increase), which was required for neutrophil recruitment after exposure to UV light. The concurrent 100- to 1,000-fold induction in the skin *g-csf* expression suggests that the IL-17A/G-CSF axis is the likely mechanism responsible for neutrophilia and neutrophil tissue homing in response to UV light. The role of IL-17A in regulating granulopoiesis and neutrophil recruitment via induction of G-CSF is well recognized under homeostatic conditions, and a few studies have identified IL-17A as important for neutrophil recruitment to the sites of sterile inflammation (41, 42). In lupus, elevated IL-17A expression is found in cutaneous lesions (43), and increased circulating IL-17A levels have been associated with worse disease manifestations (44), although the specific relationship to neutrophils, a pathogenic population in this disease (13, 17, 18), remains unexplored. Besides its direct effects on G-CSF–mediated mobilization of neutrophils from the bone marrow, IL-17A may also contribute to neutrophil homing to the kidney by stimulating expression of adhesion molecules (e.g., VCAM-1 and E-Selectin) on the renal endothelium (45, 46).

Using the same model of acute UV exposure, we recently reported that a single dose of UV light triggered a local and systemic IFN-I response, which was required for efficient neutrophil recruitment to the skin (6). Since IFN-I has been shown to induce IL-17A production (47), it is plausible that these pathways either independently or in concert lead to the UV light–mediated neutrophil recruitment and migration we report here. While our findings suggest an inflammatory role for IL-17A, suppressive effects of UVB light on IL-17A signaling have previously been reported in psoriasis, where exposure of psoriatic skin to UVB light eliminated pathogenic T cells and myeloid inflammatory dendric cells (48, 49). Since psoriatic, unlike healthy, skin is rich in IL-17–producing and –responding T cells, the difference in cellular composition is likely to determine the response to UVB light, including the extent of UVB light–mediated suppression of IL-17A receptor expression (50). UV dosage may also determine whether an inflammatory or therapeutic effect occurs: low doses are associated with anti-inflammatory and immunosuppressive consequences (51), possibly by inhibiting CD8 T cell responses (52).

Neutrophils play multiple roles during tissue inflammation. When activated by pathogen-associated molecular patterns and damage-associated molecular patterns (DAMPS) or by receptor engagement, neutrophils directly contribute to tissue injury by releasing proteases, ROS, and extrusion of neutrophil extracellular traps (NETs) (53, 54). Neutrophils can also promote tissue repair by phagocytosis of cellular debris and by enabling tissue revascularization (8). In SLE, a neutrophil gene signature is a strong predictor of active disease including LN and cutaneous lupus (17, 18). Neutrophils are found in cutaneous lesions (13, 14) as well as kidney biopsy specimens (15, 16) of SLE patients, and their inflammatory properties have been attributed, in part, to NET formation (16). This process includes increased production of ROS (55), mitochondrial DNA release (55), and release and induction of inflammatory proteins, such as s100A9 (56), IL-1b (57), and type I interferons (55, 58). Our findings that inhibiting neutrophil migration to the kidney abrogated *s100A9* and significantly reduced *IL-1b* expression and the kidney IFN score suggest that similar inflammatory functions might be at play. Relevant to kidney disease in SLE, neutrophils mainly localized to the TI endothelium, the site of increased expression of kidney injury markers *kim-1* and *lipocalin-2* in LN kidney tissues (59, 60). Proteinuria can arise due to excessive permeability of the glomerular barrier to proteins due to impaired reabsorption of protein by tubules or a combination of these mechanisms (61). TI injury in SLE patients is a frequent pathologic finding in LN kidneys, including those with mild glomerular injury (61, 62). TI injury has been shown to predict the severity of LN (63, 64), yet the mechanisms triggering it are unknown. Since elevated *kim-1* and *lipocalin-2* are recognized markers of TI injury in SLE (26, 65) and blocking neutrophil migration to the kidney inhibited their expression, we propose that the transient proteinuria observed after UV exposure is a consequence of neutrophil-mediated subclinical TI inflammation (65). Increased kidney *vcam-1* expression, another marker of TI injury in SLE (66), further supports this model.

In addition to propagating inflammation at the local sites of sterile or infectious injury, neutrophils have been shown to home to distant organs (8–10), where, depending on the context, they contribute to tissue injury via ROS production (11) or activate the adaptive immune system in the lymph nodes and the bone marrow (9, 12). The inflammatory nature of these neutrophils has been attributed to their ability to exit the primary site of injury and migrate to secondary sites, that is, to undergo rTEM (9–11, 31–34). Our findings that PA of GFP-containing cells in the skin following UV exposure led to the detection of GFP+ neutrophils in the kidney with the phenotype of rTEM suggest that a subpopulation of renal neutrophils reverse migrated from UV-exposed skin (GFP+ neutrophils make up ~20% of kidney neutrophils and of those, 20 to 35% are rTEM; therefore, rTEM make up 4 to 7% of total kidney neutrophils). This proportion of rTEM is comparable to the proportion reported after sterile liver injury (~9%) (36) and ischemia–reperfusion injury (~8%) (11). rTEM have in other circumstances been shown to be proinflammatory (10, 11) and have impaired apoptosis (35), leading to the possibility that they play a role in UV-induced kidney injury. The elevated CXCR4 expression on these neutrophils is particularly relevant, as coincident renal expression of *cxcl12*, a CXCR4 ligand expressed by podocytes and tubules (24), was observed, likely providing a chemotactic signal for this neutrophil population. Increased CXCR4 expression on immune cells coupled with high levels of renal CXCL12 have been identified in SLE patients with LN (67), and this pathway was implicated in lupus as well as ischemia–reperfusion kidney injury in mice (24, 68). In addition to being a marker of rTEM, increased CXCR4 expression is also an indicator of "aged" neutrophils, which can mediate tissue-damaging inflammatory responses (38). The precise role of CXCR4 in neutrophil recruitment to the kidney can be investigated by CXCR4 antagonism as previously done in other models of sterile injury (38).

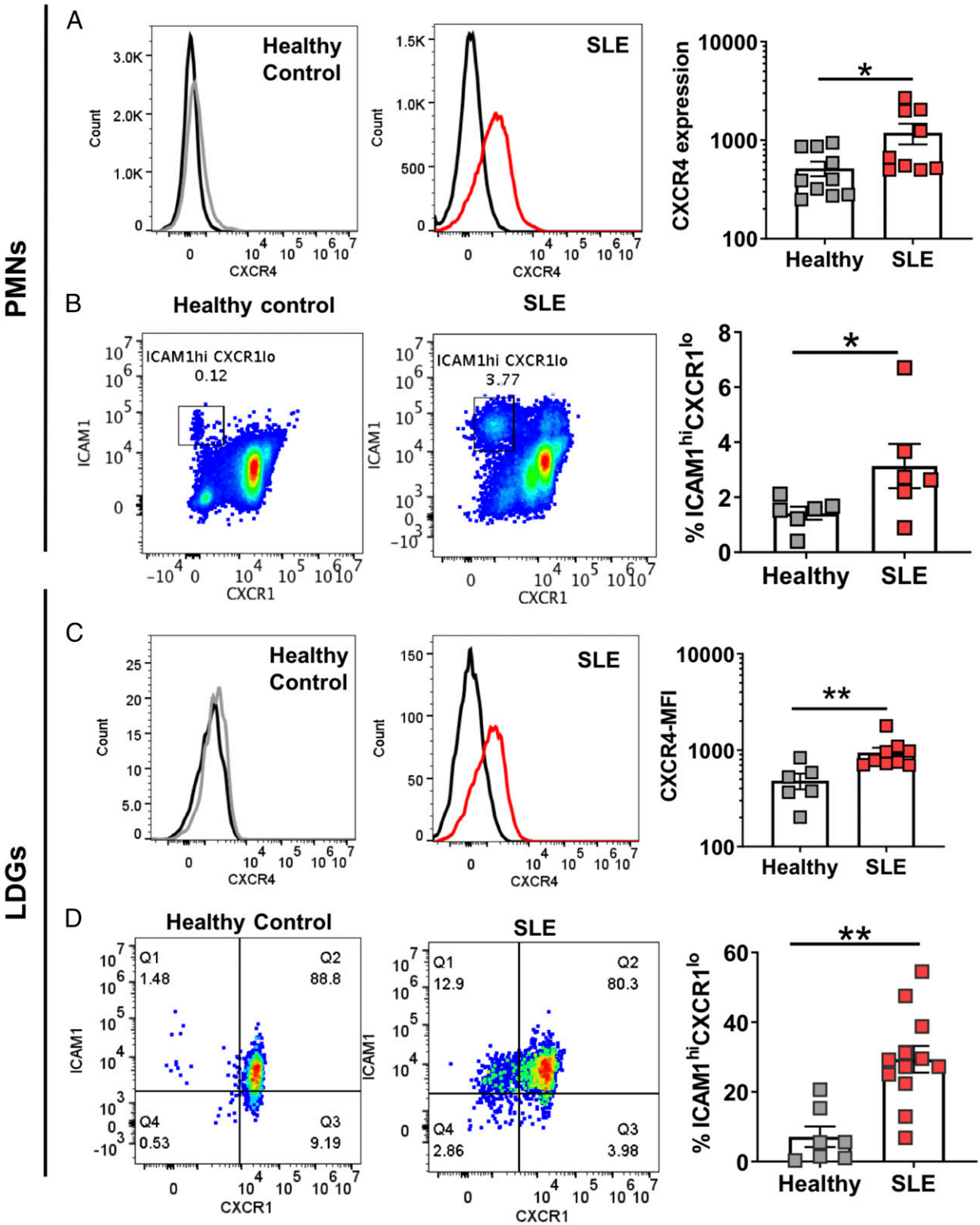

Fig. 6. Increased CXCR4 expression and presence of ICAM1^{hi}CXCR1^{lo} neutrophils (PMNs) and LDGs in SLE patients. (*A* and *C*) Mean fluorescence intensity (MFI) of CXCR4 was determined by flow cytometry analysis of (*A*) circulating PMNs (CD66b+) and (*C*) LDGs (CD10+CD15+CD14−) from healthy controls (gray) and SLE patients (red). (*B* and *D*) The percentage of ICAM1^{hi}CXCR1^{lo} cells was determined by flow cytometry of (*B*) circulating PMNs and (*D*) LDGs from healthy controls and SLE patients. Representative histograms and gates are shown. Statistical differences between groups were determined by Student's *t* test ($n = 6$ to 12; $^{*}P < 0.05$, $^{**}P < 0.01$).

Tissue-specific neutrophil migration and the mechanisms responsible for differential expression of adhesion molecules in different organs are not well understood (69). Higher levels of expression of the chemokine *cxcl12* in the kidney but not the lung could explain the preferential presence of CXCR4^{hi} neutrophils in the kidney. In addition, the induction of expression of *vcam-1*

and *e-selectin* in the kidney, compared to no change in expression in the lung, likely contributes to preferential neutrophil recruitment and retention in the kidney. The 5- to 6-fold increase in *s100A9* expression in the lung compared to a 30- to 60-fold increase in the kidney as well as a 6-fold increase in *il-1b* expression in the lung compared to 16-fold increase in the kidney further indicate tissue differences in the inflammatory response. The reduction in neutrophil infiltration of the kidney following neutralization of G-CSF can be attributed to both a reduction in circulating numbers and activation of neutrophils as well as a reduction in local expression of *vcam*-1 and *e-selectin.* However, we cannot be certain whether initial up-regulation of these adhesion molecules following skin UV exposure is attributed to skin-derived cytokines/DAMPS or whether neutrophils, through the release of serine proteases, contribute directly to their expression as has been shown in other contexts (70). Regardless of the mechanisms, and noting that we have not performed a comprehensive analysis of all tissues, our studies provide evidence for some organ selectivity in UV light–mediated systemic effects. Future studies will address tissue-specific functional consequences of systemic neutrophil dissemination by, for example, vascular albumin leakage and edema formation in the lung (11, 36).

In patients with SLE, it is difficult to unequivocally relate skin UV light exposure to exacerbations of systemic disease, as there is significant variation (1 to 3 wk) in visible photosensitivity responses in different individuals (21). In addition, subclinical kidney injury may readily be missed until consecutive exposures to UV light compound the effects. While we found that neutrophil-mediated kidney inflammation in response to UV light does not cause clinical disease in healthy mice, such a mechanism may contribute to LN flares in photosensitive lupus patients in multiple ways. Fc receptor engagement by immune complexes could enhance neutrophil recruitment, resulting in ROS and protease release (71); the heightened capacity of lupus neutrophils and LDGs to produce NETs, which, in SLE patients, are not cleared efficiently (72), could lead to the release of tissue-damaging proteases (73), propagation of the IFN-I response (58), or direct damage to the kidney endothelium by creating vascular damage and leakage (16). Moreover, the underlying differences in lupus skin, such as enhanced IFN-I signaling (5, 74) and defects in protective Langerhans cell population (75), could inform the extent and nature of neutrophil-mediated systemic responses. Tracking neutrophil migration coupled with interrogation of autoantibodies, accumulation of apoptotic cells, and low complement levels can be addressed using novel models of lupus, such as genetically defined triple mutants (*Sle1.Mfge8*$^{-/-}$ *C1q*$^{-/-}$ and *Sle1.Mfge8*$^{-/-}$*C3*$^{-/-}$) (76) or other lupus strains following exposure to UV light.

The exact mechanisms linking neutrophils to inflammation in SLE might in addition be influenced by the neutrophil/LDG phenotype, as heterogeneity within these populations has become more apparent (77). Our findings of elevated CXCR4 and ICAM1^{hi}CXCR1^{lo} (rTEM) circulating populations, particularly in SLE LDGs, further add to this heterogeneity and suggest that some of the more proinflammatory granulocytes in blood might have prior "tissue experience," that is, residence in the affected organ tissues, such as the skin, prior to systemic dissemination. The rTEM phenotypes have previously been reported in synovial fluid and circulating neutrophils of rheumatoid arthritis patients (35, 78) and in acute pancreatitis-associated lung injury (79). Their role in SLE warrants further investigation.

Materials and Methods

Mice. All animal experiments were approved by the Institutional Animal Care and Use Committee of the University of Washington, Seattle. Initial experiments were conducted using both male and female C57BL/6J mice (Jackson Laboratory, 3 to 4 mo old, Figs. 1 and 2). Female mice were used for all subsequent experiments. PA studies were performed on B6.Cg-*Ptprc*^{a} Tg(UBC-PA-GFP)1Mnz/J female mice (Jackson Laboratory, 3 to 4 mo old). These mice were generated by injection of a transgenic vector carrying PA-GFP (T203H variant) under the transcriptional control of the human ubiquitin C promoter into C57BL/6 embryos. The animals were housed in pathogen-free conditions and maintained in light–dark cycles of 12 h with ad libitum access to food and water. The experiments on all the animals were performed at the same time of the day as to avoid the influence of circadian rhythm on neutrophil migration (38).

Exposure to UVB Light and Tape Stripping. The dorsal aspect of male and female C57BL/6 mice was shaved at least 24 h prior to irradiation with UVB light, and only the mice with nonpigmented skin were used in the experiments. Mice were anesthetized with isoflurane and exposed to one dose of UVB light (500 mJ/cm^2) using FS40T12/UVB bulbs (National Biological Corporation), with peak emission between 300 and 315 nm. The UVB light energy at the dorsal surface was measured with a Photolight IL1400A radiometer equipped with a SEL240/UVB detector (International Light Technologies). Mice were euthanized 1, 2, or 6 d after exposure to UVB light, and nonirradiated mice were used as controls (D-1) (Fig. 2*A*). Epidermal tape stripping was performed as previously described (7), and skin and kidney were evaluated 24 h after injury.

Inhibition of IL-17A and G-CSF. Mice were treated intravenously with 100 μg purified rat anti-mouse IL-17A IgG (BioLegend) or isotype control 3 h before exposure to UV light (1 × 500 mJ/cm^2) (Fig. 3*I*). Neutrophil presence in the blood, skin, and saline-perfused kidney tissue was evaluated by flow cytometry 24 h after UV exposure as described below. Neutrophil migration in response to UV light was inhibited by treating mice intraperitoneally with 50 μg anti-mouse G-CSF monoclonal antibody or mouse IgG isotype control (R&D Systems) 24 h and 3 h prior to skin exposure to UVB light (1 × 500 mJ/cm^2) (Fig. 4*A*). Following cardiac perfusion, neutrophil and monocyte numbers in the kidney were evaluated by flow cytometry and gene expression by qPCR, as described below. Mice not exposed to UVB light were used as an additional control group.

Isolation of Cells from Different Organs. Following euthanasia with CO_2 inhalation, a piece of dorsal skin was removed and kept in RPMI (Roswell Park Memorial Institute) solution on ice until processing. Blood was collected by cardiac puncture in ethylenediaminetetraacetic acid-coated syringes. Cardiac perfusion was subsequently performed using phosphate-buffered saline (PBS) (~60 mL) through the left ventricle after snipping the right atrium. Successful perfusion was determined by observing complete kidney and lung pallor. Lungs, kidneys, spleen, and both femurs were removed carefully and placed in RPMI solution on ice until sample processing. Cells were isolated from equivalent areas of skin tissue (~30 mm^2) by mincing and digesting the tissue with 0.28 units/mL Liberase TM (Roche) and 0.1 mg/mL of Deoxyribonuclease I (Worthington) in PBS with Ca^{+2} and Mg^{+2} for 60 min at 37 °C with shaking. Cells were isolated from one kidney per animal; kidney tissues were minced and digested in 2 mg/mL collagenase type I (Worthington) for 30 min at 37 °C according to a published protocol. Lung cells were harvested by digesting tissue in PBS (Ca^{+2} and Mg^{+2}) with 1 mg/mL collagenase type 1 and 60 U Deoxyribonuclease I. Whole spleens were crushed onto a 40 μm cell strainer and washed with RPMI solution. Whole blood and cells from the spleen, bone marrow, kidneys, and lungs were treated with 1X Red Blood Cell (RBC) Lysis Buffer (BD Biosciences). Following isolation/digestion, cells from all tissues were filtered (40 μm), washed with PBS, and resuspended in RPMI solution prior to counting.

Flow Cytometry Staining and Analysis. Cells were treated with Fc Block TruStain FcX (Biolegend) and stained with Zombie Aqua Viability dye (Biolegend) per the vendor's recommendations. Cells were washed and surface staining was performed using mouse-specific fluorescent antibodies purchased from Biolegend. Different myeloid cell populations were analyzed in the live immune cells (Zombie Aqua-CD45+) gate. Percent and number of neutrophils (Ly6C^{int}Ly6G^{hi}) and monocytes (Ly6C+Ly6G–) were quantified. Representative flow cytometry gating is presented in *SI Appendix*, Fig. S10. Percent expression and mean fluorescence intensities of surface markers in the PA model (CXCR4, ICAM1, and CXCR1) were determined using fluorescence minus one (FMO) staining controls in the neutrophil gate (Ly6G^{hi}). All samples were processed using CytoFLEX flow cytometer (Beckman Coulter) and data analyzed with FlowJo software version 10 (Tree Star).

Photoactivation (PA) Studies. UBC-PA-GFP mice were shaved and a portion of the back was irradiated with one dose UVB light (500 mJ/cm^2) as above. Only the skin area that will be photoconverted was exposed to UVB light, while

the remaining skin was covered with aluminum foil. After 24 h from UVB-induced sterile injury, the entirety of the UVB-irradiated skin region was subjected to violet light (405 nm) using a 50 W light-emitting diode lamp with 0.37 numerical aperture (NA) fiber (Mightex) at the power of 100 mW (~15 min exposure per area). This method was optimized based on a published protocol of skin-specific photoconversion (80). Kidneys and lungs were collected and processed for flow cytometry analysis 24 h after PA, as described above. The approach and timeline are outlined in the diagram in Fig. 5*A*. The percent of GFP+ neutrophils in the kidney was compared to that found in mice under three control conditions: 1) no UV and no PA, 2) UV but no PA, and 3) no UV but PA. CXCR4 expression levels and ICAM1^{hi}CXCR1^{lo} phenotype within GFP+ and GFP− neutrophils in the skin and kidney were evaluated by flow cytometry using mouse-specific fluorescently labeled antibodies purchased from Biolegend. To determine whether the GFP+ neutrophils in the kidney originated from the skin and not blood, skin in one group of mice was exposed to UV light and PA as described above (Group I), while in another group, skin was exposed to UV light but PA was performed on the adjacent skin area not exposed to UV light (Group II) (diagram in *SI Appendix*, Fig. S7*A*). Kidneys were collected and processed for flow cytometry analysis as described above.

Gene Expression and Proteomic Analyses. Skin, kidney, and lung samples were stored in RNAlater solution (QIAGEN). RNA was extracted by RNeasy Kit from QIAGEN, and complementary DNA (cDNA) was synthesized using the High-Capacity cDNA Synthesis Kit (Applied Biosystems). The transcripts of inflammatory chemokines, cytokines, and adhesion molecules were quantified by real-time qPCR using the primers listed in *SI Appendix*, Table S1 and normalized to the average of 18S transcript levels. The dose of UVB light used did not affect 18S expression in any of the organs. Relative expression of mRNA targets was determined using the standard formula 2^(−Ct) × coefficient. IFN scores were derived from expression of 10 representative interferon-stimulated genes (ISG; *Mx1*, *Irf7*, *Isg15*, *Isg20*, *Ifi44*, *ifit1*, *ifit3*, *oasl1*, *usp18*, and *ifi27l2a*) as previously described (6). The mean and SD of the relative expression of each ISG were determined in the kidneys of mice not exposed to UV light ($mean_{noUV}$ and SD_{noUV}). These were then used to standardize the expression levels of each ISG in the kidneys of treated mice (IgG isotype + UVB or a-GCSF + UVB). The standardized expression levels were then summed for each mouse to derive an IFN expression score; i = expression of each ISG; Gene $i_{treatment}$ = relative gene expression level after treatment; and Gene i_{noUV} = relative gene expression level in mice not exposed to UVB light. $\sum_{i=1}^{10} = \frac{Genei_{treatment} - meanGenei_{noUV}}{SD(Genei_{noUV})}$.

Protein levels in plasma and skin tissue protein extracts were measured using defined analyte panels LEGENDplex Mouse Inflammation Panel and Inflammatory Chemokine Panel (Biolegend).

IF Staining of Frozen Kidney Tissues. Saline-perfused kidneys were fixed in 4% paraformaldehyde for 1 h at room temperature and, following immersion in 30% sucrose, frozen in optimal cutting medium (Sakura Finetek). The 5-μm tissue sections were rehydrated in PBS prior to IF staining. Tissues were permeabilized with 0.1% Triton X-100 in PBS and subsequently blocked in PBS + 0.1% Triton X-100/5% BSA (bovine serum albumin)/5% rabbit serum. NE and endothelial cells were detected by staining with anti-mouse NE Cy5 (1:100, Bioss) and anti-mouse PECAM-1/CD31 Al488 (1:100, Biolegend), respectively, at 4 °C overnight. Neutrophil presence in the kidney was confirmed by staining with anti-mouse Ly6G Al647 (1:100, Biolegend). Tissues were mounted using ProLong Gold with 4′,6-diamidino-2-phenylindole (DAPI) mounting medium (Invitrogen) and imaged with Nikon Eclipse 90i fluorescent microscope (Histology and Imaging Core, University of Washington).

Skin Histologic Evaluation. Formalin-fixed, paraffin-embedded skin tissue sections (4 to 5μm) were stained with hematoxylin and eosin at the University of Washington Histology and Imaging Core prior to UV, day 1, day 2, and day 6 following UVB irradiation (n = 5 females). Skin was scored in a blinded fashion for the following parameters: inflammation of the dermis/subcutis, epidermal cell death, acanthosis, hyperkeratosis, serocellular crust formation, and erosion/ulceration. These parameters were scored on a scale of 0 to 4 depending on severity and extent with the exception of erosion/ulceration, which was scored as present (1) or absent (0). Representative images were taken using NIS-Elements BR 3.2 64bit and plated in Adobe Photoshop with lighting adjustments applied to the entire image. Original magnification is stated.

Urine Measurements. Urine protein levels were evaluated by the Bradford protein assay (Thermo Fisher Scientific). Urine samples were tested at 1:40 dilution in PBS, and protein concentration in urine was determined based on serial dilutions of known concentrations of BSA. Urine albumin/creatinine ratio was evaluated by using Albuwell albumin assay and the Creatinine Companion Kit (Exocell) per the manufacturer's instructions.

Human Sample Collection and Flow Cytometry Analysis. This study was approved by the University of Washington Institution Review Board (STUDY00001145). Whole blood was collected in heparinized tubes from healthy volunteers and SLE patients following informed consent. Neutrophils (PMNs) and PBMCs were isolated by Ficoll-Paque discontinuous gradient separation (GE Healthcare). PMNs were purified from the erythrocyte pellet by 5% dextran sedimentation. Following RBC lysis, cells were stained with fluorescently labeled antibodies purchased from Biolegend, and CXCR4 expression and percent ICAM1^{hi}CXCR1^{lo} cells were evaluated in PMNs (CD66b+) and LDGs (CD15^{+}, CD14^{lo}, and CD10^{+} in PBMCs (19)). Gating strategy for LDGs and ICAM1^{hi}CXCR1^{lo} staining based on FMO is shown in *SI Appendix*, Fig. S11. Samples were processed using CytoFLEX flow cytometer (Beckman Coulter), and data were analyzed with FlowJo software version 10 (Tree Star).

Statistical Analyses. Data were analyzed using GraphPad Prism 7 software (GraphPad Software Inc.) and presented as mean ± SEM. The statistical difference between two data groups was determined relative to nonirradiated controls (D-1) using Student's t test. One-way ANOVA with multiple comparison and Tukey post hoc was used to determine the statistical significance between three groups.

Data Availability. All study data are included in the article and *SI Appendix*.

ACKNOWLEDGMENTS. This work was funded by the NIH awards R56 AR073848 (K.B.E.), T32 AR007108 (S.S.-G.), R01 AR074939 (T.M.), and R21 AR075134 (T.M.). Human studies were funded by the Institute of Translation Health Sciences Catalyst Awards, University of Washington (S.S.-G.). We thank Drs. Eric Butz, Jeffrey Ledbetter, Jessica Hamerman, Christian Lood, and Erica Noss for insightful discussion. We thank Drs. Stuart Shankland and Jonathan Himmelfarb for advice and discussion of kidney studies.

1. A. Kaul *et al.*, Systemic lupus erythematosus. *Nat. Rev. Dis. Primers* **2**, 16039 (2016).
2. E. Schmidt, H. P. Tony, E. B. Bröcker, C. Kneitz, Sun-induced life-threatening lupus nephritis. *Ann. N. Y. Acad. Sci.* **1108**, 35–40 (2007).
3. M. Barbhaiya, K. H. Costenbader, Ultraviolet radiation and systemic lupus erythematosus. *Lupus* **23**, 588–595 (2014).
4. A. Kuhn *et al.*, Photoprotective effects of a broad-spectrum sunscreen in ultraviolet-induced cutaneous lupus erythematosus: A randomized, vehicle-controlled, double-blind study. *J. Am. Acad. Dermatol.* **64**, 37–48 (2011).
5. E. Der *et al.*; Accelerating Medicines Partnership Rheumatoid Arthritis and Systemic Lupus Erythematosus (AMP RA/SLE) Consortium, Tubular cell and keratinocyte single-cell transcriptomics applied to lupus nephritis reveal type I IFN and fibrosis relevant pathways. *Nat. Immunol.* **20**, 915–927 (2019).
6. S. Skopelja-Gardner *et al.*, The early local and systemic Type I interferon responses to ultraviolet B light exposure are cGAS dependent. *Sci. Rep.* **10**, 7908 (2020).
7. C. Sontheimer, D. Liggitt, K. B. Elkon, Ultraviolet B irradiation causes stimulator of interferon genes-dependent production of protective type I interferon in mouse skin by recruited inflammatory monocytes. *Arthritis Rheumatol.* **69**, 826–836 (2017).
8. J. Wang, M. Hossain, Visualizing the function and fate of neutrophils in sterile injury and repair. *Science* **358**, 111–116 (2017).
9. H. R. Hampton, J. Bailey, M. Tomura, R. Brink, T. Chtanova, Microbe-dependent lymphatic migration of neutrophils modulates lymphocyte proliferation in lymph nodes. *Nat. Commun.* **6**, 7139 (2015).
10. C. Owen-Woods *et al.*, Local microvascular leakage promotes trafficking of activated neutrophils to remote organs. *J. Clin. Invest.* **130**, 2301–2318 (2020).
11. A. Woodfin *et al.*, The junctional adhesion molecule JAM-C regulates polarized transendothelial migration of neutrophils in vivo. *Nat. Immunol.* **12**, 761–769 (2011).
12. D. Duffy *et al.*, Neutrophils transport antigen from the dermis to the bone marrow, initiating a source of memory CD8+ T cells. *Immunity* **37**, 917–929 (2012).
13. C. C. Berthier *et al.*, Molecular profiling of cutaneous lupus lesions identifies subgroups distinct from clinical phenotypes. *J. Clin. Med.* **8**, 1244 (2019).
14. R. Safi, J. Al-Hage, O. Abbas, A. G. Kibbi, D. Nassar, Investigating the presence of neutrophil extracellular traps in cutaneous lesions of different subtypes of lupus erythematosus. *Exp. Dermatol.* **28**, 1348–1352 (2019).
15. H. Nishi, T. N. Mayadas, Neutrophils in lupus nephritis. *Curr. Opin. Rheumatol.* **31**, 193–200 (2019).
16. E. Villanueva *et al.*, Netting neutrophils induce endothelial damage, infiltrate tissues, and expose immunostimulatory molecules in systemic lupus erythematosus. *J. Immunol.* **187**, 538–552 (2011).

17. N. Jourde-Chiche *et al.*, Modular transcriptional repertoire analyses identify a blood neutrophil signature as a candidate biomarker for lupus nephritis. *Rheumatology (Oxford)* **56**, 477–487 (2017).
18. J. E. Wither *et al.*, Identification of a neutrophil-related gene expression signature that is enriched in adult systemic lupus erythematosus patients with active nephritis: Clinical/pathologic associations and etiologic mechanisms. *PLoS One* **13**, e0196117 (2018).
19. M. F. Denny *et al.*, A distinct subset of pro-inflammatory neutrophils isolated from patients with systemic lupus erythematosus induces vascular damage and synthesizes type I IFNs. *J. Immunol.* **184**, 3284–3297 (2010).
20. V. Patra, K. Wagner, V. Arulampalam, P. Wolf, Skin microbiome modulates the effect of ultraviolet radiation on cellular response and immune function. *iScience* **15**, 211–222 (2019).
21. C. J. Sanders *et al.*, Photosensitivity in patients with lupus erythematosus: A clinical and photobiological study of 100 patients using a prolonged phototest protocol. *Br. J. Dermatol.* **149**, 131–137 (2003).
22. R. J. Pepper *et al.*, S100A8/A9 (calprotectin) is critical for development of glomerulonephritis and promotes inflammatory leukocyte-renal cell interactions. *Am. J. Pathol.* **185**, 1264–1274 (2015).
23. C. W. Cheng *et al.*, Calcium-binding proteins annexin A2 and S100A6 are sensors of tubular injury and recovery in acute renal failure. *Kidney Int.* **68**, 2694–2703 (2005).
24. A. Wang *et al.*, CXCR4/CXCL12 hyperexpression plays a pivotal role in the pathogenesis of lupus. *J. Immunol.* **182**, 4448–4458 (2009).
25. M. Pitashny *et al.*, Urinary lipocalin-2 is associated with renal disease activity in human lupus nephritis. *Arthritis Rheum.* **56**, 1894–1903 (2007).
26. Y. Nozaki *et al.*, Estimation of kidney injury molecule-1 (Kim-1) in patients with lupus nephritis. *Lupus* **23**, 769–777 (2014).
27. M. R. Sharma, B. Werth, V. P. Werth, Animal models of acute photodamage: Comparisons of anatomic, cellular and molecular responses in C57BL/6J, SKH1 and Balb/c mice. *Photochem. Photobiol.* **87**, 690–698 (2011).
28. H. P. Wu *et al.*, Effect of interleukin-17 on in vitro cytokine production in healthy controls and patients with severe sepsis. *J. Formos. Med. Assoc.* **114**, 1250–1257 (2015).
29. I. K. Campbell *et al.*, Therapeutic targeting of the G-CSF receptor reduces neutrophil trafficking and joint inflammation in antibody-mediated inflammatory arthritis. *J. Immunol.* **197**, 4392–4402 (2016).
30. B. Bajrami *et al.*, G-CSF maintains controlled neutrophil mobilization during acute inflammation by negatively regulating CXCR2 signaling. *J. Exp. Med.* **213**, 1999–2018 (2016).
31. B. Colom *et al.*, Leukotriene B4-neutrophil elastase Axis drives neutrophil reverse transendothelial cell migration in vivo. *Immunity* **42**, 1075–1086 (2015).
32. J. R. Mathias *et al.*, Resolution of inflammation by retrograde chemotaxis of neutrophils in transgenic zebrafish. *J. Leukoc. Biol.* **80**, 1281–1288 (2006).
33. S. de Oliveira, E. E. Rosowski, A. Huttenlocher, Neutrophil migration in infection and wound repair: Going forward in reverse. *Nat. Rev. Immunol.* **16**, 378–391 (2016).
34. S. Nourshargh, S. A. Renshaw, B. A. Imhof, Reverse migration of neutrophils: Where, when, how, and why? *Trends Immunol.* **37**, 273–286 (2016).
35. C. D. Buckley *et al.*, Identification of a phenotypically and functionally distinct population of long-lived neutrophils in a model of reverse endothelial migration. *J. Leukoc. Biol.* **79**, 303–311 (2006).
36. J. Wang *et al.*, Visualizing the function and fate of neutrophils in sterile injury and repair. *Science* **358**, 111–116 (2017).
37. M. Yamada *et al.*, The increase in surface CXCR4 expression on lung extravascular neutrophils and its effects on neutrophils during endotoxin-induced lung injury. *Cell. Mol. Immunol.* **8**, 305–314 (2011).
38. J. M. Adrover *et al.*, A neutrophil timer coordinates immune defense and vascular protection. *Immunity* **50**, 390–402.e10 (2019).
39. K. L. Clark *et al.*, Epidermal injury promotes nephritis flare in lupus-prone mice. *J. Autoimmun.* **65**, 38–48 (2015).
40. S. J. Wolf *et al.*, TLR7-Mediated lupus nephritis is independent of type I IFN signaling. *J. Immunol.* **201**, 393–405 (2018).
41. C. M. Brackett, J. B. Muhitch, S. S. Evans, S. O. Gollnick, IL-17 promotes neutrophil entry into tumor-draining lymph nodes following induction of sterile inflammation. *J. Immunol.* **191**, 4348–4357 (2013).
42. H. Kono *et al.*, Role of IL-17A in neutrophil recruitment and hepatic injury after warm ischemia-reperfusion mice. *J. Immunol.* **187**, 4818–4825 (2011).
43. S. H. Oh *et al.*, Expression of interleukin-17 is correlated with interferon-α expression in cutaneous lesions of lupus erythematosus. *Clin. Exp. Dermatol.* **36**, 512–520 (2011).
44. M. Larosa *et al.*, IL-12 and IL-23/Th17 axis in systemic lupus erythematosus. *Exp. Biol. Med. (Maywood)* **244**, 42–51 (2019).
45. L. Roussel *et al.*, IL-17 promotes p38 MAPK-dependent endothelial activation enhancing neutrophil recruitment to sites of inflammation. *J. Immunol.* **184**, 4531–4537 (2010).
46. X. Xing *et al.*, IL-17A induces endothelial inflammation in systemic sclerosis via the ERK signaling pathway. *PLoS One* **8**, e85032 (2013).
47. P. López, J. Rodríguez-Carrio, L. Caminal-Montero, L. Mozo, A. Suárez, A pathogenic IFNα, BLyS and IL-17 axis in systemic lupus erythematosus patients. *Sci. Rep.* **6**, 20651 (2016).
48. L. M. Johnson-Huang *et al.*, Effective narrow-band UVB radiation therapy suppresses the IL-23/IL-17 axis in normalized psoriasis plaques. *J. Invest. Dermatol.* **130**, 2654–2663 (2010).
49. M. Ozawa *et al.*, 312-nanometer ultraviolet B light (narrow-band UVB) induces apoptosis of T cells within psoriatic lesions. *J. Exp. Med.* **189**, 711–718 (1999).
50. L. Yin *et al.*, Ultraviolet B inhibits IL-17A/TNF-α-Stimulated activation of human dermal fibroblasts by decreasing the expression of IL-17RA and IL-17RC on fibroblasts. *Front. Immunol.* **8**, 91 (2017).
51. G. M. Halliday, D. L. Damian, S. Rana, S. N. Byrne, The suppressive effects of ultraviolet radiation on immunity in the skin and internal organs: Implications for autoimmunity. *J. Dermatol. Sci.* **66**, 176–182 (2012).
52. S. Rana, L. J. Rogers, G. M. Halliday, Systemic low-dose UVB inhibits CD8 T cells and skin inflammation by alternative and novel mechanisms. *Am. J. Pathol.* **178**, 2783–2791 (2011).
53. J. Wang, Neutrophils in tissue injury and repair. *Cell Tissue Res.* **371**, 531–539 (2018).
54. P. H. Leliefeld, C. M. Wessels, L. P. Leenen, L. Koenderman, J. Pillay, The role of neutrophils in immune dysfunction during severe inflammation. *Crit. Care* **20**, 73 (2016).
55. C. Lood *et al.*, Neutrophil extracellular traps enriched in oxidized mitochondrial DNA are interferogenic and contribute to lupus-like disease. *Nat. Med.* **22**, 146–153 (2016).
56. H. Tydén *et al.*, Increased serum levels of S100A8/A9 and S100A12 are associated with cardiovascular disease in patients with inactive systemic lupus erythematosus. *Rheumatology (Oxford)* **52**, 2048–2055 (2013).
57. J. M. Kahlenberg, C. Carmona-Rivera, C. K. Smith, M. J. Kaplan, Neutrophil extracellular trap-associated protein activation of the NLRP3 inflammasome is enhanced in lupus macrophages. *J. Immunol.* **190**, 1217–1226 (2013).
58. G. S. Garcia-Romo *et al.*, Netting neutrophils are major inducers of type I IFN production in pediatric systemic lupus erythematosus. *Sci. Transl. Med.* **3**, 73ra20 (2011).
59. W. K. Han, V. Bailly, R. Abichandani, R. Thadhani, J. V. Bonventre, Kidney injury molecule-1 (KIM-1): A novel biomarker for human renal proximal tubule injury. *Kidney Int.* **62**, 237–244 (2002).
60. A. Viau *et al.*, Lipocalin 2 is essential for chronic kidney disease progression in mice and humans. *J. Clin. Invest.* **120**, 4065–4076 (2010).
61. A. Bökenkamp, Proteinuria-take a closer look! *Pediatr. Nephrol.* **35**, 533–541 (2020).
62. H. Lan-Ting *et al.*, Clinicopathological factors for tubulointerstitial injury in lupus nephritis. *Clin. Rheumatol.* **39**, 1617–1626 (2020).
63. C. Hsieh *et al.*, Predicting outcomes of lupus nephritis with tubulointerstitial inflammation and scarring. *Arthritis Care Res. (Hoboken)* **63**, 865–874 (2011).
64. A. Londoño Jimenez *et al.*, Brief report: Tubulointerstitial damage in lupus nephritis: A comparison of the factors associated with tubulointerstitial inflammation and renal scarring. *Arthritis Rheumatol.* **70**, 1801–1806 (2018).
65. G. S. Hill, M. Delahousse, D. Nochy, C. Mandet, J. Bariéty, Proteinuria and tubulointerstitial lesions in lupus nephritis. *Kidney Int.* **60**, 1893–1903 (2001).
66. J. Reyes-Thomas, I. Blanco, C. Putterman, Urinary biomarkers in lupus nephritis. *Clin. Rev. Allergy Immunol.* **40**, 138–150 (2011).
67. A. Wang *et al.*, Dysregulated expression of CXCR4/CXCL12 in subsets of patients with systemic lupus erythematosus. *Arthritis Rheum.* **62**, 3436–3446 (2010).
68. F. Tögel, J. Isaac, Z. Hu, K. Weiss, C. Westenfelder, Renal SDF-1 signals mobilization and homing of CXCR4-positive cells to the kidney after ischemic injury. *Kidney Int.* **67**, 1772–1784 (2005).
69. A. Margraf, K. Ley, A. Zarbock, Neutrophil recruitment: From model systems to tissue-specific patterns. *Trends Immunol.* **40**, 613–634 (2019).
70. S. J. Kuravi *et al.*, Neutrophil serine proteases mediate inflammatory cell recruitment by glomerular endothelium and progression towards dysfunction. *Nephrol. Dial. Transplant.* **27**, 4331–4338 (2012).
71. H. Nishi *et al.*, Neutrophil FcγRIIA promotes IgG-mediated glomerular neutrophil capture via Abl/Src kinases. *J. Clin. Invest.* **127**, 3810–3826 (2017).
72. A. Hakkim *et al.*, Impairment of neutrophil extracellular trap degradation is associated with lupus nephritis. *Proc. Natl. Acad. Sci. U.S.A.* **107**, 9813–9818 (2010).
73. L. J. O'Neil, M. J. Kaplan, C. Carmona-Rivera, The role of neutrophils and neutrophil extracellular traps in vascular damage in systemic lupus erythematosus. *J. Clin. Med.* **8**, 1325 (2019).
74. M. K. Sarkar *et al.*, Photosensitivity and type I IFN responses in cutaneous lupus are driven by epidermal-derived interferon kappa. *Ann. Rheum. Dis.* **77**, 1653–1664 (2018).
75. W. D. Shipman *et al.*, A protective Langerhans cell-keratinocyte axis that is dysfunctional in photosensitivity. *Sci. Transl. Med.* **10**, eaap9527 (2018).
76. S. Skopelja-Gardner *et al.*, Complement deficiencies result in surrogate pathways of complement activation in novel polygenic lupus-like models of kidney injury. *J. Immunol.* **204**, 2627–2640 (2020).
77. P. Mistry *et al.*, Transcriptomic, epigenetic, and functional analyses implicate neutrophil diversity in the pathogenesis of systemic lupus erythematosus. *Proc. Natl. Acad. Sci. U.S.A.* **116**, 25222–25228 (2019).
78. H. Brühl *et al.*, Surface expression of CC- and CXC-chemokine receptors on leucocyte subsets in inflammatory joint diseases. *Clin. Exp. Immunol.* **126**, 551–559 (2001).
79. D. Wu *et al.*, Reverse-migrated neutrophils regulated by JAM-C are involved in acute pancreatitis-associated lung injury. *Sci. Rep.* **6**, 20545 (2016).
80. M. M. Steele *et al.*, Quantifying leukocyte egress via lymphatic vessels from Murine Skin and tumors. *J. Vis. Exp.* **143**, e58704 (2019).